University of Twente

EEMCS / Electrical Engineering
Robotics and *Mechatronics*

Control Strategy for Variable Stiffness Actuators in Bilateral Teleimpedance Interaction Tasks

T.R. (Thomas) Kerkhof

MSc Report

Committee:
Prof.dr.ir. S. Stramigioli
Dr. R. Carloni
Dr. L.C. Visser
Prof.dr.ir. A. de Boer

July 2013

Report nr. 012RAM2013
Robotics and Mechatronics
EE-Math-CS
University of Twente
P.O. Box 217
7500 AE Enschede
The Netherlands

Control Strategy for Variable Stiffness Actuators in Bilateral Teleimpedance Interaction Tasks

T. R. Kerkhof

Abstract— **Teleoperated robots featuring impedance control provide a safe and flexible solution for various interaction tasks. Variable stiffness actuators cater to this control strategy with inherent mechanical impedance. This paper presents a strategy for bilateral teleimpedance control of variable stiffness actuators with the primary goal of remotely interacting with an unknown environment. Simulations and experiments on the vsaUT-II validate the control law and a haptic interface is employed to demonstrate full-system closed-loop teleoperation behaviour.**

I. INTRODUCTION

A manipulator which is controlled by a human operator from a distance potentially has many benefits over direct human manipulation, e.g. the workspace can be scaled and the operator need not be exposed to a dangerous environment. In this situation control of a vector quantity such as position, velocity or force on the robotic manipulator is inadequate as it is insufficient to control the mechanical work exchanged between the robot and its environment [1]. Instead, successful interaction with such an unknown environment requires the dynamic interaction between robot and environment to be controlled.

A method to control the dynamic behaviour of the robot is impedance control. In this method, motion is commanded and controlled and the response for deviation from that motion owing to interaction force is given in the form of an impedance [2]. It has been shown that task-dependent impedance control improves performance on manipulation tasks [3].

A way to realise impedance control is in software. This way the controller attempts to implement a dynamic relation between the manipulator variables such as position and force instead of controlling these variables alone.

Another way to achieve impedance control is to implement mechanical elastic elements. A variable stiffness actuator (VSA) consists of an output link connected to internal motors via one or more elastic elements. On top of this the effective stiffness of the elastic element(s) can be changed which allows for online control of the output stiffness. Figure 1 shows the working principle of a series VSA. Because VSA's are compliant on the mechanical level they are inherently safer than conventional actuators [4], which is why hardware impedance control is used in this research.

This work has been partly funded by the European Commissions Seventh Framework Programme as part of the project VIACTORS under grant no. 231554.

The author is with the Department of Electrical Engineering, Faculty of Electrical Engineering, Mathematics and Computer Science, University of Twente, The Netherlands (e-mail:t.r.kerkhof@student.utwente.nl)

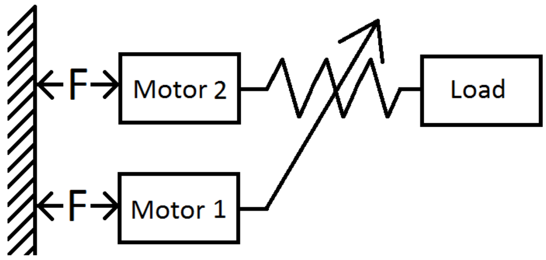

Fig. 1: Basic structure of a series VSA. Motor 1 controls the stiffness of the elastic element while motor 2 controls the equilibrium position of the load.

Controlling a VSA in free space can be done in a number of ways. Previous research has investigated classical PD-control [5] as wel as advanced techniques including feedback linearization [6]. Optimal control to optimise link velocity [7] or efficiency [8] has been studied and constrained velocity control has been used to exploit the benefits of variable stiffness independent of the specifics of the mechanical design [9]. A gain scheduling controller which ensures desired critical damping is also the subject of research [10], as is gain scheduling based on linear quadratic regulation whereby the optimal control problem is broken into linear local sub-problems and solved [11]. This has been improved by fitting a polynomial approximation on the solutions of the local sub-problems, thereby approximating the solution of the entire non-linear problem [12]. Research into interaction between a VSA and a known environment has also already been presented [13].

What is still underexposed in the current literature is the interaction between a VSA and an unknown environment. The novelty of this paper therefore lies in the constrained teleimpendance operation of a gain scheduling controlled variable stiffness actuator in interaction tasks with an unknown environment.

In this paper the autors introduce a constrained control strategy to safely establish contact with a remote unknown environment. First a feedback linearised, gain-scheduling control law is presented for a generic VSA, next a description of the vsaUT-II variable stiffness actuator is given and the controller is specified for this VSA. Simulations and experiments are used to validate this control law. Finally the controller is adopted in a bilateral teleimpedance setup and the closed loop performance of the entire system is analysed.

II. CONTROLLER DESIGN

In this section a control strategy is presented in general for any VSA with two internally actuated degrees of freedom and one output link. After that the controller parameters are specified for the vsaUT-II.

A. Feedback linearisation

A feedback loop is employed to transform the non-linear system to a linear system with the output variables as states. The simplified equations of motion for a generic VSA in free space can be given by

$$M\ddot{r} + K(q)(r - \bar{r}(q)) + D\dot{r} = 0 \tag{1}$$

$$\dot{q} = u \tag{2}$$

with M the inertia matrix, K the stiffness matrix D the viscous friction matrix, r the output position, q the internal degrees of freedom and u the input. It is assumed that the degrees of freedom of the VSA are velocity controlled, i.e. the change in stiffness is a linear function of the input vector:

$$\dot{K} = \alpha(r,q) + \beta(r,q)u$$

with $\beta = [\beta_1\ \beta_2]$ and $u = [u_1\ u_2]^T$.

Also the change in equilibrium position is assumed to be a linear function of the input vector u:

$$\dot{\bar{r}} = \gamma(r,q) + \delta(r,q)u$$

with $\delta = [\delta_1\ \delta_2]$. The system can thus be written as

$$\begin{bmatrix}\dot{\bar{r}}\\ \dot{K}\end{bmatrix} = \begin{bmatrix}\gamma\\ \alpha\end{bmatrix} + \begin{bmatrix}\delta\\ \beta\end{bmatrix} u$$

By defining the static control law

$$\begin{bmatrix}u_1\\ u_2\end{bmatrix} = \begin{bmatrix}\delta\\ \beta\end{bmatrix}^{-1} \left(- \begin{bmatrix}\gamma\\ \alpha\end{bmatrix} + \begin{bmatrix}v_r\\ v_K\end{bmatrix} \right)$$

the full form of the overall system is obtained [14]

$$\begin{bmatrix}\dot{\bar{r}}\\ \dot{K}\end{bmatrix} = \begin{bmatrix}0 & 0\\ 0 & 0\end{bmatrix} \begin{bmatrix}\bar{r}\\ K\end{bmatrix} + \begin{bmatrix}1 & 0\\ 0 & 1\end{bmatrix} \begin{bmatrix}v_r\\ v_K\end{bmatrix}$$

with v_r and v_K the new inputs of the system. This can be seen as a coordinate transformation [15]:

$$S : q \rightarrow \tilde{q}, \quad \tilde{q} := (\bar{r}, K)$$

B. Gain scheduling

The system is controlled by a state-feedback controller.

$$\begin{bmatrix}v_r\\ v_K\end{bmatrix} = G \begin{bmatrix}\bar{r}_d - \bar{r}\\ K_d - K\end{bmatrix}$$

The feedback gain matrix is given by $G = \left[\begin{smallmatrix} g_1 & 0\\ 0 & g_2\end{smallmatrix}\right]$. To achieve maximum performance g_1 will be as large as possible within certain boundaries which will be explained in the following sections. g_2 is not dependent on other states and is therefore fixed at a constant value. It is however possible to control v_K such that potential energy in the elastic elements is conserved [16]. This is however not implemented in the rest of this research.

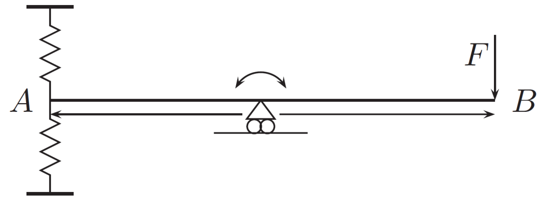

Fig. 2: Structure of the stiffness adjustment mechanism. The output stiffness K is zero when the variable pivot point is at A and it is infinite when the pivot is at B.

1) Primary Control Constraint: The main objective is to move $\bar{r}$ as fast as is physically possible, this maximum velocity will be called $\dot{\bar{r}}_{max}$. A limiting factor for this velocity might for instance be the maximum current the motor driver can deliver. The state feedback approach yields an equation of motion for $\bar{r}$:

$$\dot{\bar{r}} = -g_1(\bar{r} - \bar{r}_d) \tag{3}$$

The solution to this ODE is given by

$$\bar{r}(t) = ae^{-g_1 t}$$

In case $\bar{r}_d$ is given by a step function a is the initial difference between $\bar{r}$ and $\bar{r}_d$, also called the error. A step reference is assumed because it creates the largest possible error; it can be viewed as a worst-case scenario. $\dot{\bar{r}}_{max}$ is achieved at $t = 0$, meaning $\dot{\bar{r}}_{max} = -ag_1$. This yields the following constraint on the feedback gain.

$$g_1 \leq \left|\frac{\dot{\bar{r}}_{max}}{a}\right|$$

2) Secondary Control Constraint: The goal of the secondary constraint is to limit the oscillations of r around $\bar{r}$; a large value for g_1 gives a fast response of $\bar{r}$ but will cause large oscillations in r. Equation of motion 1 and equation 3 can be combined to yield a solution for $r(t)$, see the appendix. This equation is used to find the maximum amplitude for oscillations of r around $\bar{r}$. Assuming M and D constant, a 3-D surface describes the relation between g_1, K and the relative maximum oscillation amplitude, see figure 4. A constraint is put on this amplitude and therefore the isolines of the surface indicate maximum values of g_1 given a certain stiffness. These isolines can be parameterised to yield a numerical solution for the gain scheduling.

C. Experimental setup

The vsaUT-II realises a mechanical design which allows the apparent output stiffness to be varied by employing a lever arm with variable effective length [17]. Figure 2 shows that this is done by using a movable pivot point which changes the transmission ratio between the output and the springs. The output stiffness can be changed in a continous fashion by moving the pivot point along the entire length of the lever arm.

The position of the pivot point is defined by the internal degree of freedom q_1 which spans from 0 to L. The output stiffness K, felt at the output and associated to a force F

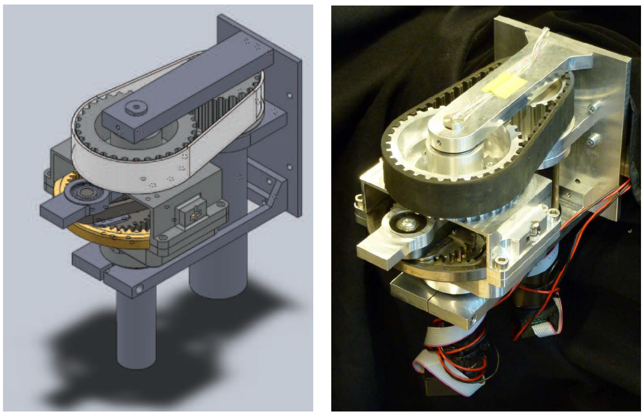

(a) CAD drawing (b) Physical prototype

Fig. 3: The vsaUT-II rotational variable stiffness actuator.

and a output deflection r is $K := \frac{\partial F}{\partial r}$ [18]. The mechanical construction of the VSA gives the following equation for the apparent output stiffness:

$$K = kL^2 \frac{(L - q_1)^2}{q_1^2} cos(2(r - q_2))$$

with k the stiffness of the internal elastic elements. This leads to

$$\begin{aligned} \dot{K} \;\; &= \;\; (-2kL^4 q_1^{-3} + 2kL^3 q_1^{-2}) cos(2r - 2q_2)\dot{q_1} - \\ & \;\;\;\; 2(kL^4 q_1^{-2} - 2kL^3 q_1^{-1} + kL^2) sin(2r - 2q_2) \end{aligned}$$

and thus

$$\begin{aligned} \alpha &= -2(kL^4 q_1^{-2} - 2kL^3 q_1^{-1} + kL^2) sin(2r - 2q_2) \\ \beta &= [(-2kL^4 q_1^{-3} + 2kL^3 q_1^{-2}) cos(2r - 2q_2) \quad 0] \end{aligned}$$

The degree of freedom q_2 defines the position of the actuator frame, i.e. the equilibrium position of the output r. If the internal springs are loaded, the output position is different than the position of the actuator frame. The equilibrium position is therefore given by $\bar{r} = q_2$, which yields

$$\dot{\bar{r}} = \dot{q}_2$$

and thus

$$\gamma = 0 \text{ and } \delta = [0 \;\; 1]$$

Further parameters for the setup are given by $M = 0.0107$ kgm^2, $D = 0.012$ Ns/m, $\dot{\bar{r}}_{max} = 0.45$ rad/s. For these values figure 4 shows the relation between the oscillation amplitude, the stiffness K and the feedback gain g_1.

III. RESULTS IN FREE SPACE

In this section results of simulations and experiments in free space, i.e. without making contact with an environment, are presented.

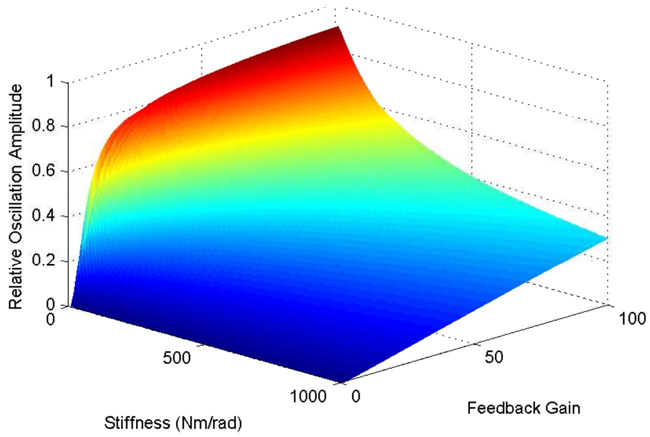

Fig. 4: Oscillation amplitude is a function of step size and feedback gain.

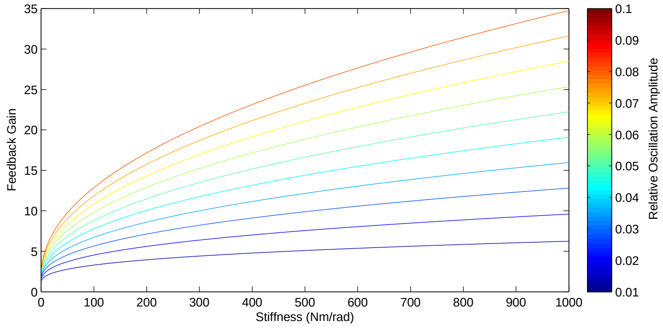

Fig. 5: When a maximum oscillation amplitude of e.g. 1% is tolerated the feedback gain is scheduled according to the corresponding -darkest blue-curve.

A. Simulations

To verify the stability of the controller the stiffness is increased alsong the entire stiffness range, from most compliant to most stiff, while a square wave is imposed on the equilibrium. The reference for the equilibrium position is a step function of 0.2 rad therefore the primary control constraint imposes a maximum feedback gain of $g_1 \leq \frac{0.45}{0.2} = 2.25$. The maximum allowable oscillation amplitude is 1%, therefore the secondary constraint follows the1%-isoline of figure 4, which is plotted in figure 5 along with other isolines. A curve is fitted along this isoline wich can be described by $g_1 \leq 0.4662K^{0.3523} + 0.9279$. The total effect of the gain scheduling is thus described by:

$$g_1(K) = \min(2.25 \;, \; 0.4662K^{0.3523} + 0.9279)$$

g_2 is set to a constant value of 1.

Figure 6a shows that for low stiffness values the oscillation amplitude is maximum 1 % due to the secondary constraint. When the stiffness is increased the primary constraint limits the equilibrium velocity and thereby also the output oscillations. The simulation is repeated for different constrained oscillation amplitudes and for different reference amplitiudes. It can be noted that the maximum oscillation amplitude and the maximum equilibrium velocity are never exceeded. Furthermore when reference profiles other than a square wave are imposed the oscillation amplitude is always

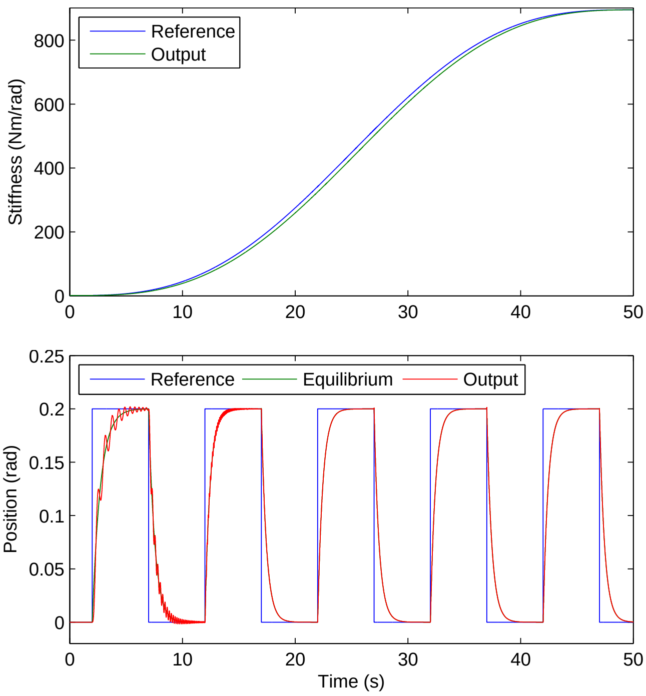

(a) Simulation results

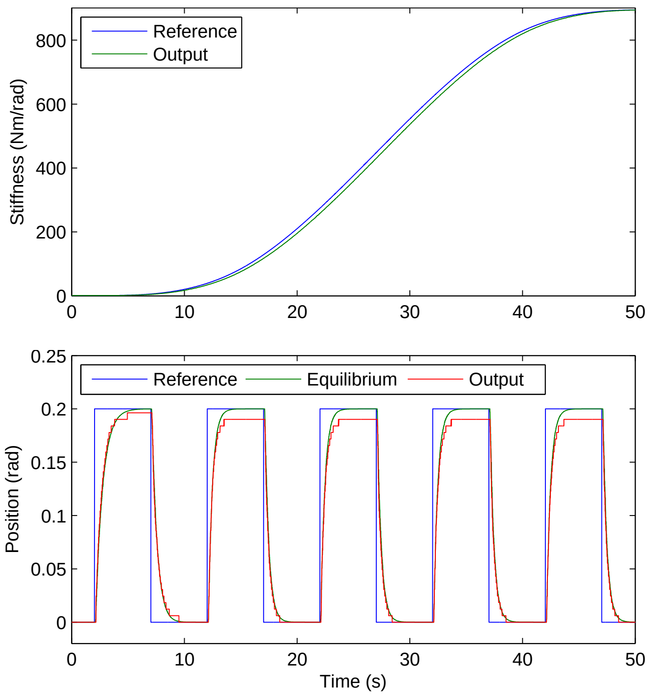

(b) Experimental results

Fig. 6: The stiffness is increased while the equilibrium positions follows a square wave reference. The controller constrains the output oscillations to 1% and the equilibrium velocity to 2.25 rad/s.

smaller as is expected considering section II-B.1.

B. Experiments

The simulated scenarios are repeated on the physical prototype of the vsaUT-II, with a maximum tolerated oscillation amplitude of 1%. A block wave reference function is imposed on the equilibrium position while the stiffness is increased along the entire stiffness range. Figure 6b shows that the stiffness and position can be independently controlled and that the system is stable for different stiffness values. Furthermore the response of the equilibrium position changes under the effect of increasing stiffness and behaves as expected. The output position follows the equilibrium, but due to the relative low encoder resolution little can be said about oscillations around the equilibrium. Also there seems to be a steady-state error at the non-zero position, this is most likely due to play in the gears and slight asymmetries in the physical realisation of the VSA.

IV. RESULTS IN CONTACT

This part discusses simulations and experiments where contact is made with an environment.

A. Simulations

The equilibrium position is moved to 0.1 rad while there is an obstacle at position $r_x = 0.05$ rad. The torque exerted on the output link is modeled with the Hunt-Crossley model [19].

$$\tau_{ext} = \begin{cases} k_{ext}(r - r_x)(t) + \lambda(r - r_x)^n(t)\dot{r}(t) & \text{for} \quad r \geq r_x \\ 0 & \text{for} \quad r < r_x \end{cases}$$

At first the stiffness is set to a low value to decrease the risk of damage to the environment and to the device. The simulation consists of three phases: first the equilibrium is moved to establish contact. After 5 seconds the stiffness is increased from 10 to 20 Nm/rad, and after 10 seconds the equilibrium position is moved back without braking contact. The results of this simulation are shown in figure 7a. When the output hits the obstacle the equilibrium continues to converge to the reference which causes the contact force to reach a steady state. When the stiffness is increased the force again converges to a steady state, and when the equilibrium is moved in the other direction the force decreases accordingly.

B. Experiments

Figure 8 shows the setup used for the experiments where contact is made.

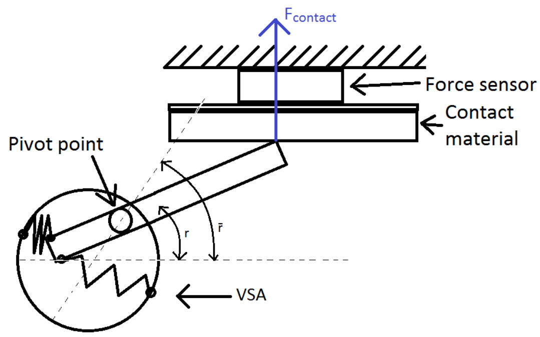

Fig. 8: Experimental setup for contact analysis

Figure 7b shows the results of the experiment where the

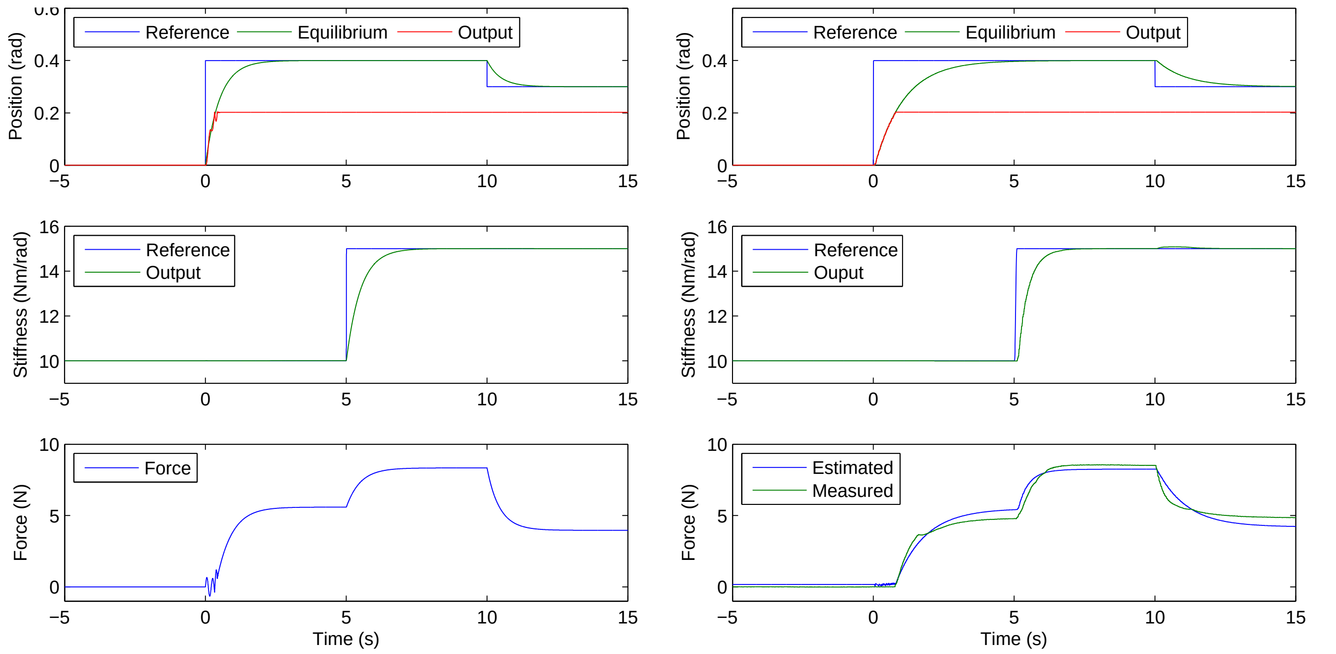

(a) Simulation results

(b) Experimental results

Fig. 7: Contact is made at low stiffness after which the stiffness is increased causing an increase in contact force. Thereafter the equilibrium is moved decreasing the force again.

output link is moved to 0.3 rad while there is an obstacle in the way. After contact is made the stiffness is increased to reach a desired impedance of 20 Nm/rad. Lastly the equilibrium moves back to 0.2 radians. The obstacle in this case is a 2 mm sheet of aluminium fixed to a force sensor (Mini40, ATI Industrial Automation, Apex, USA) which measures the normal contact force. The force is also estimated using model assumptions, in particular

$$F_{contact} = \frac{K(r - \bar{r})}{h}$$

with h the length of the output link. Is is assumed the angle of attack is 90 degrees such that the contact force equals the normal force. As the output link hits the obstacle the equilibrium continues to move, increasing the contact force. When the stiffness is increased also the force increases and when the equilibrium is moved back the force decreaes. The experimental results again closely match the simulation results.

C. Contact Material Analysis

Contact is made with different kinds of materials to test the device in different environments, in particular an aluminium plate, a piece of wood, a piece of hard Styrofoam and a piece of soft rubber foam. Initially the output stiffness is set to 10 Nm/rad and changed to 20 Nm/rad.

Figure 9 shows the reference equilibrium position, the equilibrium position and, for different environmental materials, the output position of the VSA. These different environments cause the VSA to behave in a different way, e.g. the soft foam is compressed more than the aluminium when the stiffness is increased. In all cases contact is established.

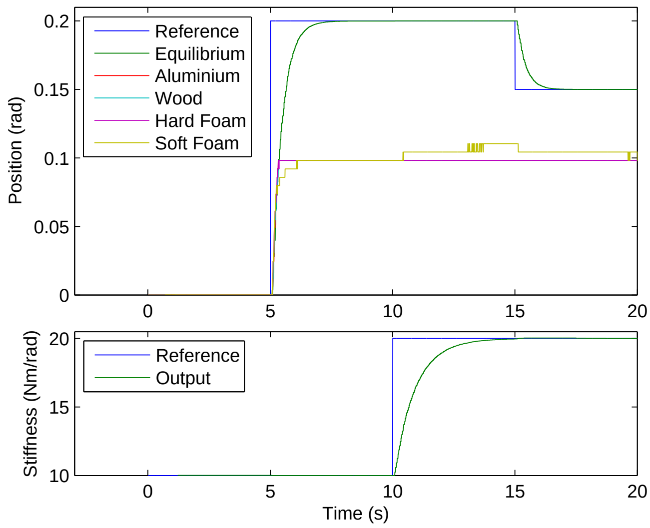

Fig. 9: Output positions for various environment materials.

V. TELEOPERATION EXPERIMENTS

This section describes methods and experiments using a bilateral teleoperation setup.

A haptic device (omega.6, Force Dimension, Nyon, Switzerland) is used to stream position and stiffness data over UDP to a Windows machine which acts as a slave controller, while force data is streamed back to the operator. The horizontal position of the haptic interface is mapped to the equilibrium position of the VSA such that it matches the translation of the tip of the manipulator. A button on the haptic interface is used to switch between a stiffness of 10

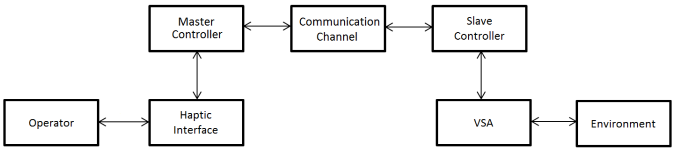

Fig. 10: Schematic representation of the control loop

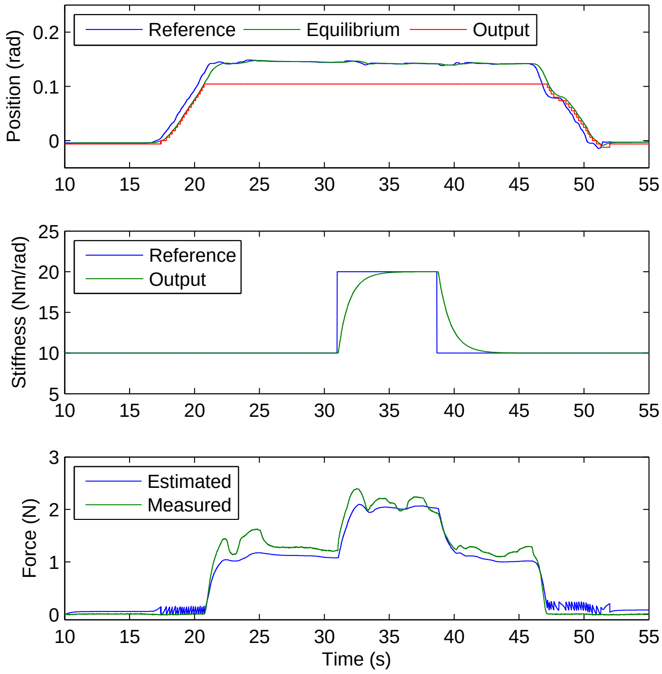

Fig. 11: Results of the haptic teleimpedance experiment as seen from the slave device.

and 20 Nm/rad. This way the operator can control stiffness and equilibrium position independently. The measured force is used purely as verification, it is the estimated force that is sent back to the haptic interface. The control parameters are given by $g_1 = \min(3, 0.4662K^{0.3523} + 0.9279)$, $g_2 = 0.5$. First contact is made with the environment -an aluminium plate- with a stiffness of 10 Nm/rad. After that the stiffness is increased to 20 Nm/rad and decreased again. Finally contact is broken and the equilibrium is moved to zero position.

Figure 11 shows that the VSA is able to follow position and stiffness references supplied by the operator and correctly relay force data back to the operator. Furthermore the closed-loop system is shown to be stable. There is however a time delay in the communication channel of approximately 1 second which decreases transparency.

VI. Conclusion

In this paper a teleimpedance control strategy for variable stiffness actuators combining constraints, feedback linearisation and gain scheduling has been presented. Simulations and experiments in both contact and non-contact, local operation and teleoperation have validated this control strategy. Interactions between the VSA and different materials have been analysed.

References

[1] N. Hogan, "Impedance control: An approach to manipulation," in *American Control Conference, 1984*, pp. 304 –313, june 1984.

[2] S. Chan, B. Yao, W. Gao, and M. Cheng, "Robust impedance control of robot manipulators.," *International Journal of Robotics & Automation*, vol. 6, no. 4, pp. 220–227, 1991.

[3] A. Blank, A. Okamura, and L. Whitcomb, "Task-dependent impedance improves user performance with a virtual prosthetic arm," in *Robotics and Automation (ICRA), 2011 IEEE International Conference on*, pp. 2235 –2242, may 2011.

[4] A. Bicchi, G. Tonietti, M. Bavaro, and M. Piccigallo, "Variable stiffness actuators for fast and safe motion control," in *Robotics Research* (P. Dario and R. Chatila, eds.), vol. 15 of *Springer Tracts in Advanced Robotics*, pp. 527–536, Springer Berlin / Heidelberg, 2005.

[5] G. Tonietti, R. Schiavi, and A. Bicchi, "Design and control of a variable stiffness actuator for safe and fast physical human/robot interaction," in *Robotics and Automation, 2005. ICRA 2005. Proceedings of the 2005 IEEE International Conference on*, pp. 526 – 531, april 2005.

[6] G. Palli, C. Melchiorri, T. Wimbock, M. Grebenstein, and G. Hirzinger, "Feedback linearization and simultaneous stiffness-position control of robots with antagonistic actuated joints," in *Robotics and Automation, 2007 IEEE International Conference on*, pp. 4367 –4372, april 2007.

[7] J. Nakanishi, K. Rawlik, and S. Vijayakumar, "Stiffness and temporal optimization in periodic movements: An optimal control approach," in *Intelligent Robots and Systems (IROS), 2011 IEEE/RSJ International Conference on*, pp. 718 –724, sept. 2011.

[8] M. Garabini, A. Passaglia, F. Belo, P. Salaris, and A. Bicchi, "Optimality principles in variable stiffness control: The VSA hammer," in *Intelligent Robots and Systems (IROS), 2011 IEEE/RSJ International Conference on*, pp. 3770 –3775, sept. 2011.

[9] M. Howard, D. Braun, and S. Vijayakumar, "Constraint-based equilibrium and stiffness control of variable stiffness actuators," in *Robotics and Automation (ICRA), 2011 IEEE International Conference on*, pp. 5554–5560, 2011.

[10] A. Albu-Schaffer, S. Wolf, O. Eiberger, S. Haddadin, F. Petit, and M. Chalon, "Dynamic modelling and control of variable stiffness actuators," in *Robotics and Automation (ICRA), 2010 IEEE International Conference on*, pp. 2155–2162, 2010.

[11] D. Braun, F. Petit, F. Huber, S. Haddadin, P. van der Smagt, A. Albu-Schaffer, and S. Vijayakumar, "Optimal torque and stiffness control in compliantly actuated robots," in *Intelligent Robots and Systems (IROS), 2012 IEEE/RSJ International Conference on*, pp. 2801–2808, IEEE, 2012.

[12] I. Sardellitti, G. Medrano-Cerda, N. Tsagarakis, A. Jafari, and D. Caldwell, "Gain scheduling control for a class of variable stiffness actuators based on lever mechanisms," *Robotics, IEEE Transactions on*, vol. PP, no. 99, pp. 1–7, 2013.

[13] B.-S. Kim and J.-B. Song, "Object grasping using a 1 dof variable stiffness gripper actuated by a hybrid variable stiffness actuator," in *Robotics and Automation (ICRA), 2011 IEEE International Conference on*, pp. 4620 –4625, may 2011.

[14] G. Palli, C. Melchiorri, and A. De Luca, "On the feedback linearization of robots with variable joint stiffness," in *Robotics and Automation, 2008. ICRA 2008. IEEE International Conference on*, pp. 1753 –1759, may 2008.

[15] L. C. Visser, S. Stramigioli, and A. Bicchi, "Embodying desired behavior in variable stiffness actuators," in *Proceedings of the 18th IFAC World Congress, 2011*, no. 1, (Milan, Italy), pp. 9733–9738, IFAC, August 2011.

[16] L. C. Visser, R. Carloni, and S. Stramigioli, "Energy efficient control of robots with variable stiffness actuators," in *Proceedings of the 8th IFAC Symposium on Nonlinear Control Systems, NOLCOS 2010, Bologna, Italy*, 2010.

[17] S. Groothuis, G. Rusticelli, A. Zucchelli, S. Stramigioli, and R. Carloni, "The vsaUT-II: A novel rotational variable stiffness actuator," in *Robotics and Automation (ICRA), 2012 IEEE International Conference on*, pp. 3355 –3360, may 2012.

[18] S. Groothuis, G. Rusticelli, A. Zucchelli, S. Stramigioli, and R. Carloni, "The variable stiffness actuator vsaUT-II: Mechanical design, modeling, and identification," 2013.

[19] K. H. Hunt and F. R. E. Crossley, "Coefficient of restitution interpreted as damping in vibroimpact," *Journal of Applied Mechanics*, vol. 42, pp. 440–445, june 1975.

Appendix

Combining the equation of motion 1 with equation 3 yields the following solution

$$
\begin{aligned}
r(t) &= \frac{aKe^{-g_1 t}}{-Dg + g^2 M + K} + c_1 e^{\frac{-t\sqrt{D^2-4MK}-D}{2M}} \\
&+ c_2 e^{\frac{t\sqrt{D^2-4MK}-D}{2M}}
\end{aligned}
$$

Setting $r(0) = a$ and $\dot{r}(0) = 0$ the integration constants become

$$
\begin{aligned}
c_1 &= a - v - \frac{g_1 v - \frac{-\sqrt{D^2-4MK}-D}{2M} a + \frac{-\sqrt{D^2-4MK}-D}{2M} v}{\frac{\sqrt{D^2-4MK}-D}{2M} - \frac{-\sqrt{D^2-4MK}-D}{2M}} \\
c_2 &= \frac{g_1 v - \frac{-\sqrt{D^2-4MK}-D}{2M} a + \frac{-\sqrt{D^2-4MK}-D}{2M} v}{\frac{\sqrt{D^2-4MK}-D}{2M} - \frac{-\sqrt{D^2-4MK}-D}{2M}}
\end{aligned}
$$

with a the initial position of both r and $\bar{r}$ with respect to $\bar{r}_d$.